The EMBO Journal Vol. 21 No. 9 pp. 2198–2206, 2002

tcBid promotes Ca^{2+} signal propagation to the mitochondria: control of Ca^{2+} permeation through the outer mitochondrial membrane

György Csordás, Muniswamy Madesh, Bruno Antonsson[1] and György Hajnóczky[2]

Department of Pathology, Anatomy and Cell Biology, Thomas Jefferson University, Philadelphia, PA 19107, USA and [1]Department of Protein Biochemistry, Serono Pharmaceutical Research Institute, CH-1228 Geneva, Switzerland

[2]Corresponding author
e-mail: Gyorgy.Hajnoczky@mail.tju.edu

Calcium spikes established by IP_3 receptor-mediated Ca^{2+} release from the endoplasmic reticulum (ER) are transmitted effectively to the mitochondria, utilizing local Ca^{2+} interactions between closely associated subdomains of the ER and mitochondria. Since the outer mitochondrial membrane (OMM) has been thought to be freely permeable to Ca^{2+}, investigations have focused on IP_3-driven Ca^{2+} transport through the inner mitochondrial membrane (IMM). Here we demonstrate that selective permeabilization of the OMM by tcBid, a proapoptotic protein, results in an increase in the magnitude of the IP_3-induced mitochondrial $[Ca^{2+}]$ signal. This effect of tcBid was due to promotion of activation of Ca^{2+} uptake sites in the IMM and, in turn, to facilitation of mitochondrial Ca^{2+} uptake. In contrast, tcBid failed to control the delivery of sustained and global Ca^{2+} signals to the mitochondria. Thus, our data support a novel model that Ca^{2+} permeability of the OMM at the ER–mitochondrial interface is an important determinant of local Ca^{2+} signalling. Facilitation of Ca^{2+} delivery to the mitochondria by tcBid may also support recruitment of mitochondria to the cell death machinery.

Keywords: apoptosis/Bid/calcium/mitochondria/outer mitochondrial membrane

Introduction

Early studies with isolated mitochondria established the dogma that the outer mitochondrial membrane (OMM) allows free passage of Ca^{2+} (for references see Mannella, 1992). Thus Ca^{2+} transport through the inner mitochondrial membrane (IMM) mediated by an electrogenic uniport emerged as the sole determinant of mitochondrial Ca^{2+} uptake. Although the Ca^{2+} uptake sites in the IMM exhibit relatively low affinity for Ca^{2+}, inositol trisphosphate (IP_3) receptor- and ryanodine receptor-driven cytosolic $[Ca^{2+}]$ ($[Ca^{2+}]_c$) spikes that peak at <1 μM are delivered effectively to the mitochondria (Rizzuto *et al*., 1993). Recently, it has been demonstrated that propagation of the $[Ca^{2+}]_c$ spikes to the mitochondria is facilitated by a local Ca^{2+} control between IP_3/ryanodine receptors and the mitochondrial uptake sites at closely apposed domains of the endoplasmic reticulum (ER) and mitochondria (Rizzuto *et al*., 1998; Csordás *et al*., 1999). The ER–mitochondrial communication is likely to be supported by physical links between the two organelles (Frey and Mannella, 2000; Wang *et al*., 2000) and displays a functional organization similar to synapses (Csordás *et al*., 1999). However at the ER–mitochondrial interface, the OMM is inserted between what would be pre- and postsynaptic structures. If the regions of the OMM between the interfacing ER Ca^{2+} release channels and uptake sites are not freely permeable, mitochondrial Ca^{2+} uptake sites may fail to sense the transient, high $[Ca^{2+}]_c$ microdomain in the vicinity of the activated IP_3/ryanodine receptors. Thus, the presence of structures that ensure free passage of Ca^{2+} through the OMM is of critical importance at the ER–mitochondrial interface.

Ca^{2+} may traverse the OMM through the pores formed by the voltage-dependent anion channel (VDAC) (reviewed in Mannella, 1992). In particular, the closed conformation of the VDAC shows cation selectivity (Benz and Brdiczka, 1992). Interestingly, at the contact sites, the VDAC is envisaged to interact with an IMM transporter, the adenine nucleotide translocator (ANT), to form the permeability transition pore (PTP) complex, and this complex may promote Ca^{2+} release from the mitochondria under physiological and pathophysiological conditions (Ichas and Mazat, 1998; Bernardi, 1999; Crompton, 1999; Hajnóczky *et al*., 2000). However, it is unclear whether the VDACs also form complexes with the IMM Ca^{2+} uniporters, which may facilitate mitochondrial Ca^{2+} uptake. In addition to the OMM permeability established by the VDAC, Bcl-2 family proteins induce a large increase in the permeability of the OMM during apoptosis (Green and Reed, 1998; Vander Heiden and Thompson, 1999; Desagher and Martinou, 2000; Korsmeyer *et al*., 2000; Kroemer and Reed, 2000). This is due to an interaction between proapoptotic (e.g. Bid, Bad, Bak and Bax) and antiapoptotic (Bcl-2 and Bcl-x_L) proteins in the mitochondrial membrane, and this interaction may also involve the VDAC (Shimizu *et al*., 1999) or ANT (Marzo *et al*., 1998a). The increased OMM permeability allows for the release of large proteins from the intermembrane space to the cytosol [cytochrome *c* (Liu *et al*., 1996), apoptosis-inducing factor (Susin *et al*., 1999a), caspases (Krajewski *et al*., 1999; Samali *et al*., 1999; Susin *et al*., 1999b), Smac/DIABLO (Du *et al*., 2000; Verhagen *et al*., 2000), endonuclease G (Li *et al*., 2001)]. So Ca^{2+} may certainly traverse the newly formed holes in the OMM. In many apoptotic paradigms, the PTP opening results in permeabilization of the IMM simultaneously with the OMM (Marchetti *et al*., 1996; Lemasters *et al*., 1998; Marzo *et al*., 1998b; Scorrano *et al*., 2001) but, in other models, selective permeabilization of the OMM occurs and the IMM damage is delayed (e.g. von Ahsen *et al*., 2000;

Mootha *et al*., 2001; Waterhouse *et al*., 2001). We thought that investigation of the effect of selective OMM permeabilization on the IP_3-induced $[Ca^{2+}]_m$ rise may allow us to revisit the role of OMM permeability in the control of calcium signal propagation from ER to mitochondria in the cells.

In response to engagement of the death receptors, a BH3-only Bcl-2 family protein, Bid, is cleaved by caspase-8 and, subsequently, the truncated C-terminus Bid (tcBid) induces release of apoptotic factors from mitochondria (Li *et al*., 1998; Luo *et al*., 1998; Gross *et al*., 1999). tcBid has been demonstrated to translocate from cytosol to the mitochondria (Li *et al*., 1998; Luo *et al*., 1998; Gross *et al*., 1999), and to exhibit high affinity for the lipid domains of the OMM at the contact sites (Lutter *et al*., 2000, 2001). Studies with different experimental systems have resulted in numerous mechanisms that may mediate tBid-induced cytochrome *c* release. These include ion channel activity (Schendel *et al*., 1999), destabilization of the lipid bilayer by tcBid on its own (Kudla *et al*., 2000) and interaction of tBid with proapoptotic Bcl-2 family proteins [Bax (Wang *et al*., 1996; Desagher *et al*., 1999; Eskes *et al*., 2000) and Bak (Wei *et al*., 2000)] or components of the PTP (Zamzami *et al*., 2000). Although the exact mechanism underlying tcBid-induced membrane permeabilization remains elusive, several reports showed that the IMM barrier function is maintained during tcBid-induced release of apoptotic factors from the mitochondria (e.g. von Ahsen *et al*., 2000; Mootha *et al*., 2001; Waterhouse *et al*., 2001). Here we first show that tcBid evokes selective permeabilization of the OMM in permeabilized RBL-2H3 cells that we have established previously as a model for local Ca^{2+} signalling between IP_3 receptors and mitochondria (Csordás *et al*., 1999; Pacher *et al*., 2000). We show that treatment with tcBid promotes propagation of the IP_3-induced $[Ca^{2+}]_c$ signal to the mitochondria. In contrast, we find that tcBid does not affect the $[Ca^{2+}]_m$ rise during sustained and global $[Ca^{2+}]_c$ elevations. From our data, a novel model emerges that the permeability of the OMM limits the delivery of IP_3-linked $[Ca^{2+}]_c$ spikes and oscillations to the mitochondria. This is because the short-lasting high $[Ca^{2+}]_c$ microdomains in the vicinity of IP_3 receptors require free passage of Ca^{2+} through the OMM to establish optimal activation of the mitochondrial Ca^{2+} uptake sites. Interestingly, an increase in the OMM permeability also delays the deactivation of the Ca^{2+} uptake sites during IP_3-induced Ca^{2+} release. Thus our study confirms that the OMM permits Ca^{2+} delivery to the IMM during sustained $[Ca^{2+}]_c$ elevations, but challenges the freely Ca^{2+}-permeable model of the OMM and reveals an important role for the OMM in the local control of Ca^{2+} signalling between ER and mitochondria.

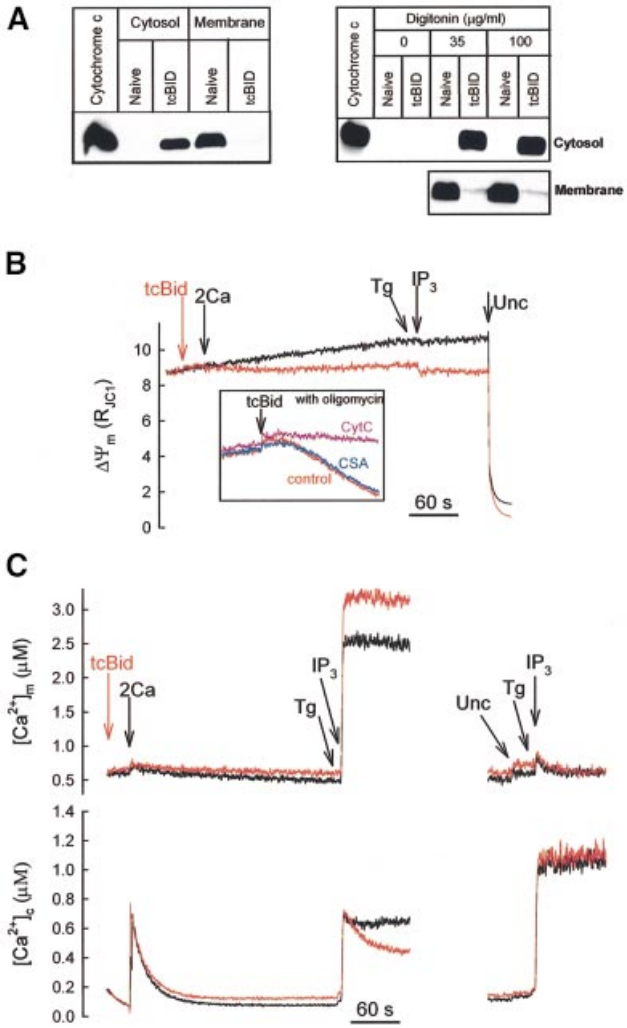

Fig. 1. tcBid induces selective permeabilization of the OMM and promotes propagation of the IP_3-induced $[Ca^{2+}]_c$ signal to the mitochondria in suspensions of permeabilized RBL-2H3 cells. (**A**) The permeabilized cells were treated with tcBid (200 nM for 5 min) or solvent, then centrifuged, and the supernatants (cytosol) and pellets (membrane) were resolved by 15% SDS–PAGE followed by immunoblotting for cytochrome *c* (left panel). To evaluate the respective roles of cell permeabilization and tcBid in cytochrome *c* release, cells were exposed to varying concentrations of digitonin for 5 min prior to treatment with solvent or tcBid (100 nM for 5 min) (right panel). (**B**) $\Delta\Psi_m$ was monitored in suspensions of permeabilized cells incubated in the presence of tcBid (red) or solvent (black). Additions were: tcBid (200 nM), $CaCl_2$ (2 μM, 2Ca), IP_3 (10 μM) and uncoupler (Unc; FCCP/oligomycin 5 μg/ml of each). Inset: tcBid (20 nM)-induced mitochondrial depolarization in the presence of oligomycin. Incubations were carried out in the presence of cytochrome *c* (10 μM; purple trace), cyclosporin A (5 μM; blue trace) or solvent (red trace). (**C**) Cytosolic $[Ca^{2+}]$ was followed with rhod2/FA added to the medium (lower panel) and $[Ca^{2+}]_m$ was measured using compartmentalized fura2FF (upper panel). tcBid- (200 nM), $CaCl_2$- (2 μM, 2Ca) and IP_3- (10 μM) induced $[Ca^{2+}]_c$ and $[Ca^{2+}]_m$ responses were recorded in the absence or presence of uncoupler (Unc; FCCP/oligomycin 5 μg/ml of each). The data are representative of 3–7 different experiments.

Results and discussion

Permeabilization of the OMM by tcBid enhances the IP_3-induced $[Ca^{2+}]_m$ signal

Recent evidence suggests that tcBid associates with the OMM at the contact sites (Lutter *et al*., 2000, 2001), evokes selective permeabilization of the OMM and, in turn, cytochrome *c* release (Li *et al*., 1998; Luo *et al*., 1998; Gross *et al*., 1999). We speculated that tcBid may allow us to determine whether propagation of $[Ca^{2+}]_c$ signals into the mitochondria is limited by the Ca^{2+} permeability of the OMM in the cells. Treatment of digitonin-permeabilized RBL-2H3 cells with tcBid (200 nM for 5 min) resulted in redistribution of cytochrome *c* from mitochondria to the cytosol (Figure 1A, left), indicating permeabilization of the OMM. Notably, incubation of the

cells with digitonin *per se* caused permeabilization of the plasma membrane (<5% Trypan Blue exclusion), but did not evoke cytochrome *c* release (Figure 1A, right). The OMM barrier resisted even a 3-fold higher concentration of digitonin (Figure 1A, right). Furthermore, in the absence of digitonin, treatment with tcBid did not result in cytochrome *c* redistribution from mitochondria to the cytosol (Figure 1A, right), suggesting that tcBid did not permeabilize the plasma membrane and OMM in intact cells.

Although depletion of mitochondrial cytochrome *c* inhibits the respiratory chain activity, if the IMM is intact, generation of $\Delta\Psi_m$ may be maintained at the expense of added ATP. Measurements of $\Delta\Psi_m$ confirmed that tcBid elicited only a small depolarization when mitochondria were energized with 2 mM succinate (complex II substrate) in the presence of 2 mM MgATP (Figure 1B, compare with the complete depolarization induced by uncoupler). In contrast, the $\Delta\Psi_m$ dissipated rapidly if tcBid was added to cells pre-treated with an inhibitor of the F_1F_0-ATPase, oligomycin (5 μg/ml) (Figure 1B, inset). The oligomycin-dependent depolarization was inhibited effectively by exogenous cytochrome *c* (20 μM), illustrating that depletion of cytochrome *c* accounted for the depolarization (Figure 1B, inset). Notably, tcBid-induced mitochondrial depolarization was not inhibited by cyclosporin A (5 μM), an agent that abolished the loss of $\Delta\Psi_m$ mediated by opening of the PTP complex (n = 2, not shown). These results show that exposure to tcBid evoked permeabilization of the OMM, whereas the integrity of the IMM was preserved in RBL-2H3 cells. After cytochrome *c* depletion, reverse operation of the mitochondrial F_1F_0-ATPase allowed for generation of $\Delta\Psi_m$.

Simultaneous measurements of $[Ca^{2+}]_c$ and $[Ca^{2+}]_m$ (Figure 1C, left) showed that IP_3-induced Ca^{2+} release evoked a $[Ca^{2+}]_c$ rise (lower part) closely followed by a $[Ca^{2+}]_m$ increase (upper traces). The global $[Ca^{2+}]_c$ increase caused by IP_3 was similar to the effect of 2 μM $CaCl_2$, whereas only IP_3 evoked a large $[Ca^{2+}]_m$ response, illustrating the effective delivery of IP_3-induced Ca^{2+} release to the mitochondria, that has been shown to be due to a local Ca^{2+} transfer between IP_3 receptors and mitochondrial Ca^{2+} uptake sites (Rizzuto *et al.*, 1998; Csordás *et al.*, 1999). Addition of tcBid (200 nM) did not change the basal $[Ca^{2+}]_c$ or $[Ca^{2+}]_m$ much, and did not affect the initial $[Ca^{2+}]_c$ elevation evoked by IP_3, but caused a marked increase in the $[Ca^{2+}]_m$ rise (Figure 1C, left, upper red versus black traces). On average, the $[Ca^{2+}]_m$ signal was increased by 19.5 ± 4.2% (n = 7, P <0.01). Notably, tcBid also accelerated the decay of the IP_3-induced $[Ca^{2+}]_c$ rise (Figure 1C, left, lower red versus black traces) and this effect could not result from a rapid reuptake of released Ca^{2+} to the ER, since IP_3 was added together with the ER Ca^{2+} pump inhibitor, thapsigargin (Tg). However, this experiment could not exclude the possibility that tcBid affected IP_3-induced Ca^{2+} mobilization from the ER. To further discriminate between potential effects of tcBid on ER and mitochondrial Ca^{2+} handling, we repeated the above experiment in the presence of uncoupler (FCCP + oligomycin) that eliminated the driving force of mitochondrial Ca^{2+} uptake. The IP_3-induced $[Ca^{2+}]_c$ rise was enhanced and the $[Ca^{2+}]_m$ rise was abolished by the uncoupler (Figure 1C, right, black traces). Under these conditions, tcBid failed to change the $[Ca^{2+}]_c$ and $[Ca^{2+}]_m$ responses (red traces), suggesting that tcBid did not affect Ca^{2+} release from the ER and that the above-described effects of tcBid resulted from changes in mitochondrial Ca^{2+} handling. Furthermore, a change in the IP_3 sensitivity could not account for any effects of tcBid, since a maximal dose of IP_3 (10 μM) was used in all studies. One might also speculate whether the electron transport chain inhibition (Figure 1B) could account for the effects of tcBid on the $[Ca^{2+}]$ signal. However when we supplemented the medium with cytochrome *c* (20 μM) to rescue the electron transport chain activity or we added a complex III inhibitor, antimycin A (5 μM), tcBid could still accelerate the decay of the IP_3-induced $[Ca^{2+}]_c$ signal (n = 2, not shown). Most recently, tcBid has also been reported to trigger reorganization of the IMM, and this process was inhibited by cyclosporin A (Scorrano *et al.*, 2002). Thus it is important to note that in our study, the effect of tcBid on the IP_3-induced calcium signals was not inhibited by cyclosporin A (5 μM, n = 2).

Taken together, these observations suggest that tcBid selectively permeabilized the OMM and the effect of tcBid on the mitochondria yielded enhanced delivery of the IP_3-driven $[Ca^{2+}]_c$ signal to the mitochondria. Since tcBid caused a small depolarization in our experiments (Figure 1B), the $\Delta\Psi_m$ component of the driving force of Ca^{2+} uptake was decreased rather than increased. This decrease in the driving force of the mitochondrial Ca^{2+} uptake was significant, because when we used a low dose of uncoupler (FCCP, 20 nM) to establish a depolarization comparable with the effect of tcBid, we noted significant inhibition of mitochondrial Ca^{2+} uptake during IP_3-induced Ca^{2+} mobilization (n = 3, not shown). Thus, the enhanced IP_3-induced $[Ca^{2+}]_m$ signal in tcBid-pre-treated cells could be due to the fact that the permeabilized OMM optimized delivery of the localized Ca^{2+} release to the mitochondrial Ca^{2+} uptake sites located in the IMM. This could augment the $[Ca^{2+}]$ gradient between the two sides of the IMM, increasing the driving force of Ca^{2+} uptake. In addition, Ca^{2+} could exert an allosteric control on the Ca^{2+} uptake sites, increasing the Ca^{2+} permeability of the IMM. It was also possible that tcBid released a negative modulator of the sites that mediate Ca^{2+} uptake through the IMM.

In addition to the studies with tcBid, we also investigated whether Bax, another proapoptotic Bcl-2 family protein, induces cytochrome *c* release and increases the IP_3-induced $[Ca^{2+}]_m$ signals. The oligomeric form of Bax (500 nM) evoked cytochrome *c* release in permeabilized RBL-2H3 cells, but >30 min incubation was required to obtain a release similar to that evoked by tcBid (n = 3, data not shown). Because the local Ca^{2+} coupling between ER and mitochondria is not preserved for so long after cell permeabilization, we could perform a 5–7 min preincubation with Bax before addition of IP_3. Under these conditions, only a relatively small cytochrome *c* release and no increase in the IP_3-induced $[Ca^{2+}]_m$ signal were observed (n = 3, data not shown).

tcBid fails to affect the $[Ca^{2+}]_m$ response evoked by sustained and global $[Ca^{2+}]_c$ signals

During IP_3-induced Ca^{2+} release, due to local interactions between ER and mitochondria, subdomains of the mitochondrial surface could be exposed to a high $[Ca^{2+}]$

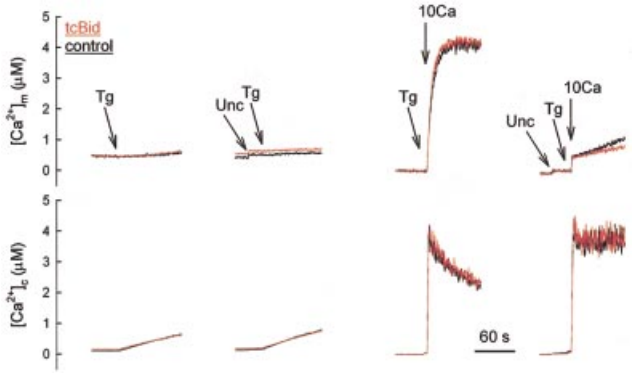

Fig. 2. No effect of tcBid on delivery of Tg- and Ca^{2+}-induced sustained $[Ca^{2+}]_c$ signals to the mitochondria. Cytosolic $[Ca^{2+}]$ was followed with rhod2/FA added to the medium (lower panel) and $[Ca^{2+}]_m$ was measured using compartmentalized fura2FF (upper panel). tcBid (200 nM, red) or solvent (black) was added to the permeabilized cells 5 min before treatment with either Tg (2 μM) or $CaCl_2$ (10 μM, 10Ca) in the absence or presence of uncoupler (Unc; FCCP/oligomycin 5 μg/ml of each). These data are representative of three different experiments.

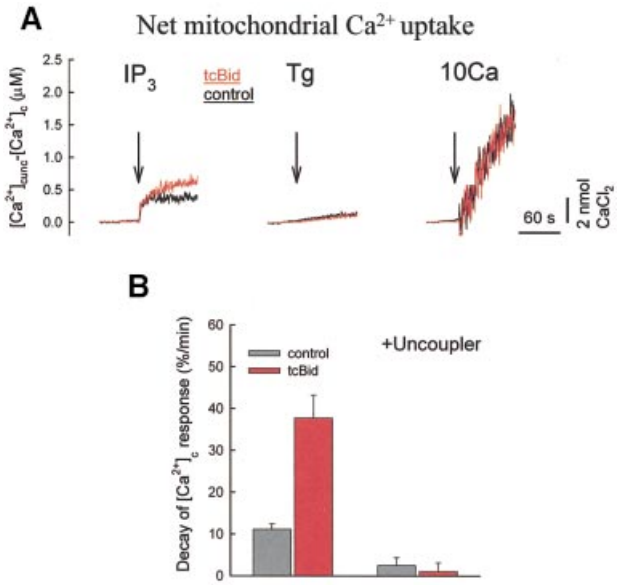

Fig. 3. tcBid enhances the net mitochondrial Ca^{2+} uptake evoked by IP_3-induced Ca^{2+} release. (**A**) Net mitochondrial Ca^{2+} uptake evoked by IP_3 (10 μM), Tg (2 μM) and $CaCl_2$ (10 μM, 10Ca) in the absence (black traces) and presence of tcBid (200 nM, red traces). To calculate net mitochondrial Ca^{2+} accumulation, the IP_3-induced $[Ca^{2+}]_c$ signal was subtracted from a parallel experiment carried out in the presence of uncoupler. The traces represent mean values calculated for experiments performed with 3–7 different cell cultures (IP_3, seven; Tg, three; and 10Ca, three), and each experiment was carried out in duplicate. (**B**) Rate of mitochondrial Ca^{2+} uptake during IP_3-induced Ca^{2+} mobilization in the absence (black) or presence of tcBid (red). Decay of the global $[Ca^{2+}]_c$ signal (60 s) was normalized to the initial peak value as follows: decay rate (%/min) = $\{([Ca^{2+}]_{c\text{-peak}} - [Ca^{2+}]_{c\text{-60 s}})/[Ca^{2+}]_{c\text{-peak}}\} \times 100$. Calculations were carried out with the data obtained in the absence (left) and presence of uncoupler. The data represent means ± SE from seven different experiments.

microdomain that decays very quickly to the level of the measured global $[Ca^{2+}]_c$ as the ER becomes depleted. Thus, high Ca^{2+} permeability of the OMM could be critical in activation of mitochondrial Ca^{2+} uptake by the short-lasting high Ca^{2+} microdomain. However, enhancement of the permeability of the OMM by tcBid may be less important for mitochondrial Ca^{2+} uptake evoked by sustained $[Ca^{2+}]_c$ elevations. We observed that the Tg-induced gradual depletion of the ER store resulted in a slow $[Ca^{2+}]_c$ rise (Figure 2, left, lower part) associated with a delayed and very small $[Ca^{2+}]_m$ increase (Figure 2, left, upper part). Neither the $[Ca^{2+}]_c$, nor the $[Ca^{2+}]_m$ response was modified by tcBid (Figure 2, left). We also established a sustained $[Ca^{2+}]_c$ elevation to ~3 μM by addition of 10 μM $CaCl_2$ (Figure 2, right). Again, tcBid pre-treatment did not augment the $[Ca^{2+}]_m$ response (Figure 2, right, upper part). Furthermore, when a $[Ca^{2+}]_c$ rise similar to the IP_3-induced elevation of global $[Ca^{2+}]_c$ (~0.7–1 μM) was established by addition of 2–3 μM $CaCl_2$, only a slow and small $[Ca^{2+}]_m$ rise occurred that was not increased by tcBid ($n = 3$, not shown). Thus, the basal Ca^{2+} permeability of the OMM was sufficient to allow activation of the Ca^{2+} uptake sites in the IMM by the sustained $[Ca^{2+}]_c$ increases. Since tcBid failed to augment the Tg- and Ca^{2+}-induced Ca^{2+} rise, it is unlikely that tcBid promoted the effect of IP_3 by releasing a negative modulator of the Ca^{2+} uptake sites.

tcBid enhances the net mitochondrial Ca^{2+} uptake evoked by IP_3

The $[Ca^{2+}]_m$ response reflects the combined effects of the mitochondrial Ca^{2+} uptake, intramitochondrial Ca^{2+} buffering and Ca^{2+} efflux from the mitochondria. To evaluate the net mitochondrial Ca^{2+} uptake in the case of each stimulus (IP_3, Tg and Ca^{2+} addition), we calculated the difference of the $[Ca^{2+}]_c$ signals obtained in the presence and absence of uncoupler (Figure 3A). During IP_3-induced Ca^{2+} release, a net mitochondrial Ca^{2+} uptake was apparent immediately and increased further for a short time period (left, black trace). In the presence of tcBid, the IP_3-induced Ca^{2+} uptake was larger than in naive cells, in particular, the sustained phase was augmented and prolonged (red trace). With regard to evaluation of the time course of the IP_3 effect, it is also worthy of note that the initial upstroke is very sensitive to the temporal alignment of the two records of $[Ca^{2+}]_c$ used for the calculation (+ and – uncoupler), and so evaluation of the initial phase is not as accurate as that of the sustained phase. In the case of Tg and Ca^{2+}, the net mitochondrial Ca^{2+} uptake gradually increased over a relatively long time period and no effect of tcBid appeared (middle and right, black versus red traces). Thus, permeabilization of the OMM by tcBid augmented only the IP_3-induced mitochondrial Ca^{2+} uptake. The effect of tcBid on the mitochondrial Ca^{2+} uptake was quantitated by calculation of the decay rate of the IP_3-induced $[Ca^{2+}]_c$ rise that was recorded as shown in Figure 1C, left (Figure 3B). On average, the mitochondrial Ca^{2+} uptake rate was increased from 11.1 ± 1.3 to 37.7 ± 5.5%/min in tcBid-pre-treated cells ($n = 7$, $P < 0.005$).

tcBid augmented both the $[Ca^{2+}]_m$ rise and mitochondrial Ca^{2+} uptake during IP_3-induced Ca^{2+} mobilization, but the maximal effect on $[Ca^{2+}]_m$ took place in <20 s, whereas the effect on net mitochondrial Ca^{2+} uptake developed for >30s. Based on the above studies and on the Mn^{2+} quench measurements (Figure 4), during the initial phase of Ca^{2+} release, a relatively small increase in IMM Ca^{2+} permeability and mitochondrial Ca^{2+} uptake was

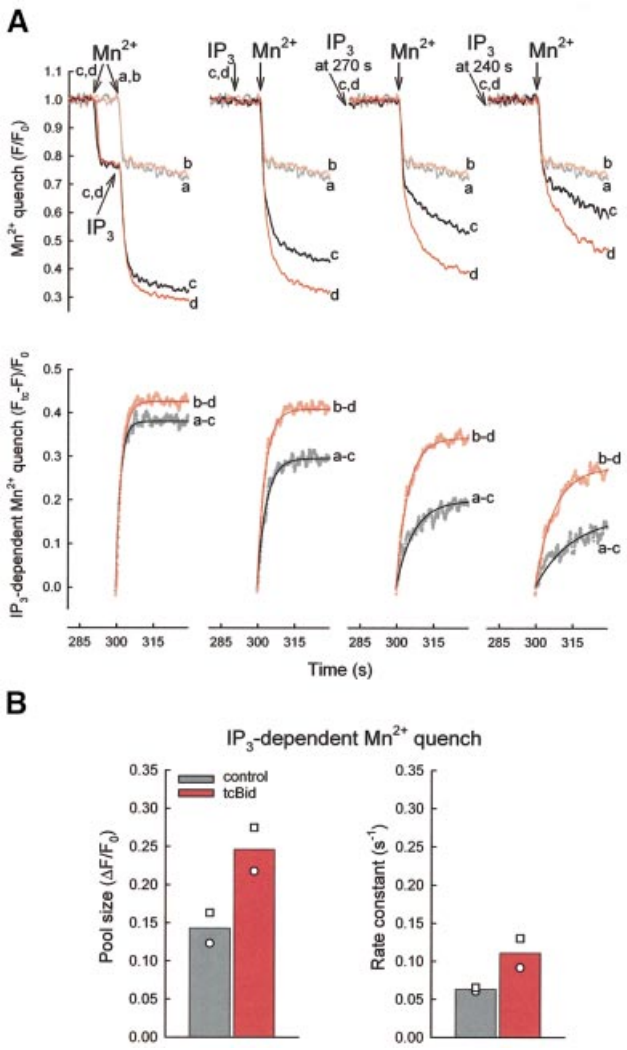

Fig. 4. tcBid facilitates the effect of IP_3 on permeability of the mitochondrial Ca^{2+} uptake sites. (**A**) Fluorescence quenching was initiated by addition of 50 μM $MnCl_2$ (Mn^{2+}) to fura2FF-loaded permeabilized cells. Permeabilized cells were pre-treated with tcBid (200 nM for 5 min, traces b and d) or solvent (traces a and c). The traces show: no IP_3 addition (a and b), IP_3 added (c and d) 10 s after Mn^{2+} (left), 10 s (290 s, middle left), 30 s (270 s, middle right) and 60 s (240 s, right) before Mn^{2+}, respectively. Fura2FF fluorescence (F) was normalized to the initial fluorescence (F_0). The free Mn^{2+} (~3 μM, buffered by ATP) exceeds the K_d for Mn^{2+} binding to fura2FF by 2–3 orders of magnitude, which ensures essentially stochiometric quench of compartmentalized fura2FF as Mn^{2+} enters the mitochondrial matrix. In the lower row, the IP_3-dependent component of the Mn^{2+} quench responses was obtained by subtraction from a parallel quench response in the absence of IP_3 (–tcBid, a–c; +tcBid, b–d), and non-linear regression (single exponential) fits were calculated for the first 30 s after Mn^{2+} addition (solid lines). (**B**) Pool size and rate constant calculated for the IP_3-dependent Mn^{2+} quench obtained in the absence (grey) and presence of tcBid (red). Calculations were carried out using the traces shown in (A, lower row). Thus, the pool size of the IP_3-dependent Mn^{2+} quench is expressed as a fraction of the initial fluorescence ($\Delta F/F_0$). The rate constant was calculated for a 30 s period (from 300 to 330 s, Mn^{2+} added at 300 s) and is expressed as s^{-1} Bi-exponential kinetics appeared to provide a better fit to a few recordings of Mn^{2+} quench in control cells pre-treated with IP_3 for 30 and 60 s, but for calculation of the rate constants we used the single exponential kinetic that gave an excellent fit to most of the traces. The symbols show the results with two different cell cultures; each experiment was carried out in duplicate.

sufficient to augment the $[Ca^{2+}]_m$ response to IP_3, whereas the sustained increase in Ca^{2+} permeability and mitochondrial Ca^{2+} uptake did not enhance the $[Ca^{2+}]_m$ signal further. An important consideration is that the mitochondrial Ca^{2+} efflux mechanisms exhibit very low activity in RBL-2H3 cells as compared with cardiac myotubes and hepatocytes (Csordás *et al.*, 1999; Pacher *et al.*, 2000). Thus a sustained modest increase in mitochondrial Ca^{2+} influx may result in a progressive increase in the net mitochondrial Ca^{2+} uptake. However, the sustained increase in mitochondrial Ca^{2+} uptake was not associated with a progressive increase in $[Ca^{2+}]_m$. One clue to this is that up-regulation of mitochondrial Ca^{2+} buffering has been reported during Ca^{2+} uptake to the mitochondria (David, 1999). We speculate that the sustained component of mitochondrial Ca^{2+} uptake failed to increase $[Ca^{2+}]_m$ further due to an increase in the Ca^{2+} buffer species. For example, mitochondrial Ca^{2+} uptake is associated with phosphate uptake that may account for a gradual increase in Ca^{2+} buffering capacity.

We also noted that in tcBid-treated cells, the IP_3-dependent net mitochondrial Ca^{2+} uptake was sustained (>30 s), even though the net Ca^{2+} efflux from the ER decayed in <5 s (calculated as the first derivative of the $[Ca^{2+}]_c$ signal, not shown) and the high Ca^{2+} microdomain could not be maintained after cessation of the Ca^{2+} release. However, Ca^{2+} has been shown to exert a slow allosteric control on mitochondrial Ca^{2+} uptake sites *in vitro* (Kröner, 1986) as well as *in vivo* (Hajnóczky *et al.*, 1995). Recent evidence also suggests that ryanodine receptors may mediate mitochondrial Ca^{2+} uptake in cardiac muscle (Beutner *et al.*, 2001), supporting the view that Ca^{2+}-gated Ca^{2+} channels may serve as Ca^{2+} uptake sites in the IMM (Litsky and Pfeiffer, 1997). Thus the initial $[Ca^{2+}]_c$ rise could establish sensitization/activation of the Ca^{2+} uptake sites, allowing for some Ca^{2+} uptake after the dissipation of the high $[Ca^{2+}]$ microdomain. Furthermore, the tcBid-induced permeabilization of the OMM could evoke a large increase (>3-fold) of this effect.

tcBid facilitates the effect of IP_3 on permeability of the mitochondrial Ca^{2+} uptake sites

To follow the effect of tcBid on the net conductance of the mitochondrial Ca^{2+} uptake sites throughout extended periods of IP_3 exposure, we developed a method using Mn^{2+} as a Ca^{2+} surrogate to examine the permeability of the mitochondrial Ca^{2+} uptake sites. In RBL-2H3 cells, we could load the mitochondria with fura2FF that shows several hundred-fold higher affinity towards Mn^{2+} than Ca^{2+} and was almost completely quenched by Mn^{2+}. It has also been shown that Mn^{2+} can enter the mitochondria through the Ca^{2+} uptake sites (Vinogradov and Scarpa, 1973; Gunter and Pfeiffer, 1990; Gunter *et al.*, 1994). The Mn^{2+} quench experiments were carried out using an excitation wavelength of 357 nm, where fura2FF is insensitive to $[Ca^{2+}]$ changes. Addition of Mn^{2+} to the permeabilized cells resulted in a prompt quench of released cytosolic fura2FF (~20%), followed by a slow basal quench of the compartmentalized dye (Figure 4A, traces a). Approximately 60% of the compartmentalized fura2FF was quenched rapidly when IP_3 was added (Figure 4A, left, trace c). However, IP_3 failed to induce

Mn^{2+} quench if: (i) the ER Ca^{2+} store was depleted by Tg; (ii) the $\Delta\Psi_m$ was dissipated by FCCP or antimycin; or (iii) the IMM Ca^{2+} uptake sites were inhibited by ruthenium red (2 μM) prior to IP_3 addition (not shown). These data show that the IP_3-dependent Mn^{2+} quench was triggered by the Ca^{2+} release and that Mn^{2+} acted as a Ca^{2+} surrogate, passing through the Ca^{2+} uniporter. Since Mn^{2+} quenches fura2FF in an essentially stochiometric manner until the dye becomes saturated, the rate of Mn^{2+} quench can be used as a measure of the net permeability properties of the mitochondrial Ca^{2+} uptake sites. To examine the permeability properties of the Ca^{2+} uniporter after various periods of IP_3 exposure, Mn^{2+} was added to permeabilized cells pre-incubated in the presence of IP_3 for 10, 30 and 60 s, respectively (Figure 4A, left to right). As illustrated by the c traces (shown in black), the rate and magnitude of the Mn^{2+} quench displayed a monotonic decrease with the time of IP_3 pre-treatment, suggesting that the IP_3-induced enhancement of the Mn^{2+} permeability decayed gradually.

Pre-treatment with tcBid did not change the Mn^{2+} quench rate in the absence of IP_3 (Figure 4A, left, trace b versus trace a), suggesting that permeabilization of the outer membrane by itself did not affect Ca^{2+} entry through the IMM. However, the IP_3-dependent Mn^{2+} quench of compartmentalized fura2FF was enhanced by tcBid (traces d versus traces c) particularly at 30 and 60 s after IP_3 addition (Figure 4A, right). To visualize the tcBid-induced changes better, the IP_3-dependent component of Mn^{2+} quench was obtained for each time point by subtraction of the trace recorded in the presence of IP_3 from a parallel quench response in the absence of IP_3 and, subsequently, non-linear regression analysis was carried out (Figure 4A, lower panel: –tcBid, a–c; + tcBid, b–d). The IP_3-induced Mn^{2+} quench followed single exponential kinetics, and the pool size as well as the rate constant was increased by tcBid (Figure 4B). These results provide direct evidence that permeabilization of the OMM by tcBid facilitated the activation of the Ca^{2+} uptake sites in the IMM during IP_3-induced Ca^{2+} release. The tcBid-induced sustained increase in IP_3-dependent Mn^{2+} quench provides a mechanism that underlies the sustained stimulation of IP_3-dependent Ca^{2+} uptake to the mitochondria (Figure 3). Facilitation of the transmission of the Ca^{2+} signal from the IP_3 receptors to the IMM by tcBid enhances rapid activation of the Ca^{2+} uptake sites. Furthermore, a slower decay from the relatively high initial activity results in prolonged stimulation of the mitochondrial Ca^{2+} uptake. The OMM permeabilization by tcBid is likely to facilitate the Ca^{2+} uptake sites by optimizing the exposure of the allosteric Ca^{2+}-binding site to the high local $[Ca^{2+}]_c$ rise, since reproduction of the IP_3-induced global $[Ca^{2+}]_c$ increase (~0.7–1 μM) by addition of 2–3 μM $CaCl_2$ yielded only a very small increase in the Mn^{2+} quench rate (data not shown).

Localization of the holes in OMM controls the IP_3-induced mitochondrial calcium signal

Release of apoptotic proteins is likely to occur through OMM pores distributed throughout the entire mitochondrial surface. However, to support a local Ca^{2+} signal transmission, the OMM pores should be positioned precisely between the IP_3 receptors and IMM Ca^{2+} uptake sites at the interfacing domains of the ER and mitochondria. Assuming that the number of sites of OMM permeabilization is proportional to the concentration of tcBid but each pore permeates cytochrome *c* and Ca^{2+}, one can speculate whether depletion of cytochrome *c* requires less tcBid than facilitation of delivery of the IP_3-induced Ca^{2+} signal to the mitochondria. As shown in Figure 5A, 2 nM tcBid evoked substantial cytochrome *c* release and 5 nM caused an almost maximal release response. In contrast, no enhancement of the IP_3-induced $[Ca^{2+}]_m$ rise or stimulation of mitochondrial Ca^{2+} uptake was elicited by 2 and 5 nM tcBid (Figure 5B). The promotion of IP_3-induced mitochondrial calcium signalling was noted at 20 nM tcBid and maximal response was achieved using 200 nM tcBid (Figure 5B). Thus, despite the relatively small size of Ca^{2+}, facilitation of Ca^{2+} signal propagation to the mitochondria requires more extensive permeabilization of the OMM than cytochrome *c* release. This is consistent with the idea that a few, randomly distributed pores are sufficient to allow release of mitochondrial factors from the intermembrane space to the cytosol, whereas strategic localization of the OMM pores to the space between interacting ER and IMM Ca^{2+} transporters is required to support recognition of the highly localized and transient ER Ca^{2+} release by the mitochondria.

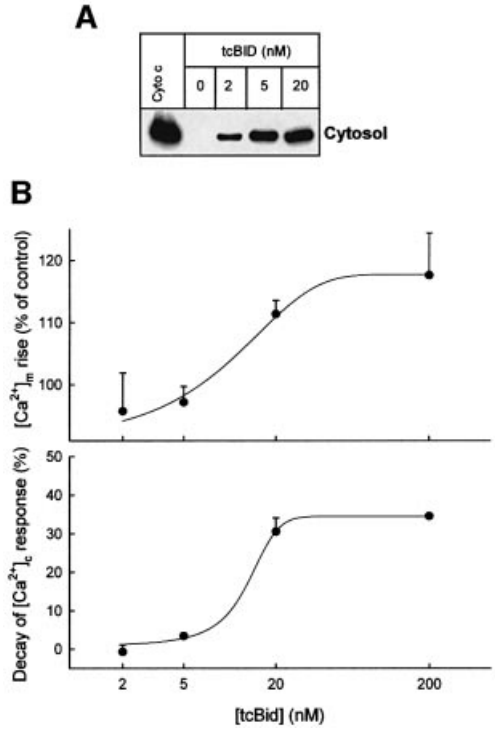

Fig. 5. Local calcium signalling is less sensitive than cytochrome *c* release to tcBid, suggesting a role for targeting of the OMM pores to the ER–mitochondrial interface. (**A**) Dose–response for cytochrome *c* release evoked by tcBid. Cytosolic samples were generated by rapid filtration of the cells. The data are representative of two different experiments. (**B**) Dose–response for tcBid-induced potentiation of the IP_3-dependent $[Ca^{2+}]_m$ signal (upper) and for enhancement of the mitochondrial Ca^{2+} uptake rate (lower). The data represent means ± SE from 3–5 experiments.

Taken together, the present experiments showed that exposure to tcBid enhanced the OMM permeability without destroying the IMM barrier. Since we observed bi-directional passage of cytochrome *c* through the OMM, it is likely that the OMM also permitted free translocation

of Ca^{2+} in tcBid-treated cells. Our data also showed that exposure to tcBid promoted Ca^{2+} signal propagation to the mitochondria. This did not reflect an effect of tcBid on the ER Ca^{2+} store, since tcBid failed to affect IP_3- or Tg-induced Ca^{2+} release from the ER (Figures 1C and 2) and augmented the IP_3-induced $[Ca^{2+}]_m$ signal when ER Ca^{2+} uptake was inhibited (Figure 1C). Then we evaluated whether permeabilization of the OMM or another effect on the mitochondria accounts for tcBid-induced facilitation of mitochondrial Ca^{2+} signalling. For example, tcBid might release a negative modulator of the Ca^{2+} uptake sites from the intermembrane space, but we showed that tcBid did not affect the propagation of global and sustained $[Ca^{2+}]_c$ signals to the mitochondria (Figure 2). It was also unlikely that tcBid augmented the driving force of mitochondrial Ca^{2+} uptake as the $\Delta\Psi_m$ was slightly attenuated in tcBid-treated cells (Figure 1B). Thus we thought that stimulation of local Ca^{2+} delivery to the mitochondria was due to the permeabilization of the OMM or to a shortening of the distance between ER and Ca^{2+} uptake sites in the IMM. However, electron microscopic and electron tomography analysis did not show a tcBid-induced change in the shape of the mitochondrial surface (von Ahsen *et al*., 2000) and the Tg-induced mitochondrial Ca^{2+} signalling was not affected by tcBid (Figures 2 and 3), arguing against the idea that tcBid brought the ER and mitochondria closer to each other. Thus we propose that facilitation of mitochondrial Ca^{2+} signalling took place because tcBid evoked selective permeabilization of the OMM. This model challenges the dogma that the OMM is freely permeable to Ca^{2+}. However, the 'leaky OMM' was envisaged based on studies that were carried out with isolated mitochondria, and the OMM permeability could have changed during the preparation of mitochondria. Furthermore, the local $[Ca^{2+}]_c$ signals delivered from IP_3 receptors to the mitochondria in the cells decay very quickly, underscoring the requirement for a very effective transfer between IP_3 receptors and the Ca^{2+} uptake sites in the IMM. Since tcBid seems to interact selectively with the OMM at the contact sites (Lutter *et al*., 2000), we postulate that the contact site regions at the ER–mitochondrial interface may be particularly important in local Ca^{2+} signalling. In the contact site regions, the tight association between the OMM and IMM narrows the gap between IP_3 receptors and mitochondrial Ca^{2+} uptake sites. Finally, evaluation of the decay phase of the IP_3-induced $[Ca^{2+}]_c$ signal and the Mn^{2+} quench measurements allowed us to establish the kinetics of the Ca^{2+} uptake sites during IP_3-induced Ca^{2+} release (Figures 3 and 4). The initial large activation was augmented in the presence of tcBid but, more strikingly, the deactivation was slowed down, suggesting that the initial exposure to the high Ca^{2+} microdomain controlled the lifetime of the activated conformation of the Ca^{2+} uptake sites.

Conclusions

Our study demonstrated that transport of Ca^{2+} through the OMM limits propagation of Ca^{2+} spikes to the mitochondria. Although the Ca^{2+} permeability of the OMM is sufficient to ensure optimal activation of the Ca^{2+} uniporter during sustained $[Ca^{2+}]_c$ signals, the OMM attenuates exposure of the Ca^{2+} uptake sites to the short-lasting, high $[Ca^{2+}]_c$ microdomains generated by the neighbouring IP_3 receptors. Under physiological conditions, Ca^{2+} transport through the OMM is likely to be mediated by the pores formed by the VDACs (Mannella, 1992). Thus, changes in the level of expression, spatial distribution or activity of VDACs may affect the delivery of Ca^{2+} spikes to the mitochondria. Recently, Rosario Rizzuto's group provided direct evidence that overexpression of the VDAC facilitates Ca^{2+} signal propagation to the mitochondria (E.Rapizzi, P.Pinton, G.Vandecasteele, G.Szabadkai, K.E. Fogarty and R.Rizzuto, submitted). In line with our results, overexpression of the VDAC promoted IP_3 receptor-driven mitochondrial Ca^{2+} signalling but failed to affect the $[Ca^{2+}]_m$ rise evoked by capacitative Ca^{2+} entry or global $[Ca^{2+}]_c$ elevation (E.Rapizzi, P.Pinton, G.Vandecasteele, G.Szabadkai, K.E.Fogarty and R.Rizzuto, submitted). Since the IP_3 receptor-driven mitochondrial Ca^{2+} uptake is an important regulator of mitochondrial ATP production and also exerts feedback control on cytosolic Ca^{2+} signalling, VDAC-dependent changes in the local Ca^{2+} control between ER and mitochondria may affect many cellular functions. During apoptosis, if tcBid-induced permeabilization of the OMM does not cause dissipation of the $\Delta\Psi_m$ (Waterhouse *et al*., 2001), facilitation of mitochondrial Ca^{2+} uptake may result in mitochondrial Ca^{2+} overload. This may evoke PTP-mediated Ca^{2+}-induced Ca^{2+} release that in turn recruits the neighbouring mitochondria (Ichas *et al*., 1997), providing a mechanism that may also contribute to the coordinated execution of the mitochondrial phase of cell death (Pacher and Hajnóczky, 2001). Future studies will address whether tcBid interacts with VDACs to increase the OMM Ca^{2+} permeability or if channel-forming Bcl-2 family proteins create the molecular structures that support an increase in Ca^{2+} transport at the contact sites.

Materials and methods

Recombinant protein

Caspase 8-cleaved Bid (tcBid) and oligomeric Bax were produced as described earlier (Desagher *et al*., 1999; Antonsson *et al*., 2001).

Fluorometric measurements of $[Ca^{2+}]_c$, $[Ca^{2+}]_m$, Mn^{2+} quench and $\Delta\Psi_m$ in suspensions of permeabilized cells

RBL-2H3 cells were cultured, loaded with fura2FF for measurements of $[Ca^{2+}]_m$, permeabilized with digitonin using a protocol that preserves the functional integrity of the calcium coupling between ER and mitochondria, and incubated as described earlier (Csordás *et al*., 1999; Csordás and Hajnóczky, 2001). Briefly, fura2FF-loaded cells (5.5×10^6 cells/ml) were permeabilized in an intracellular medium (ICM) composed of 120 mM KCl, 10 mM NaCl, 1 mM KH_2PO_4, 20 mM Tris–HEPES, 2 mM MgATP, 5% dextran and 1 μg/ml each of antipain, leupeptin and pepstatin at pH 7.2 supplemented with 25–35 μg/ml digitonin [Sigma, 50% (w/w)] for 5 min at 35°C, followed by washout of the released cytosolic fura2FF (125 g for 4 min). Cell permeabilization was evaluated by Trypan Blue exclusion and, after 5 min incubation, >95% of the cells were Trypan positive. Compartmentalized fura2FF has been shown to occur in the mitochondria of RBL-2H3 cells (Csordás *et al*., 1999). Permeabilized cells were resuspended in ICM supplemented with 2 mM succinate and 0.25 μM rhod2/FA and maintained in a stirred thermostated cuvette at 35°C. Rhod2/FA was added to monitor $[Ca^{2+}]$ in the intracellular medium that exchanges readily with the cytosolic space. Fluorescence was monitored in a multiwavelength excitation dual-wavelength emission fluorimeter using 340 nm, 380 nm excitation and 500 nm emission for fura2FF, and 540 nm excitation and 580 nm emission for rhod2. In every experiment, five data triplets were obtained per second. Calibration of the Ca^{2+} signals was carried out at the end of each measurement as described previously (Csordás and Hajnóczky, 2001). In the Mn^{2+} quench experiments, excitation of fura2FF was also

carried out at 357 nm (five data points/s), where the fura2FF fluorescence was insensitive to Ca^{2+} changes. At the end of each Mn^{2+} quench measurement, a high concentration of Mn^{2+} (500 μM $MnCl_2$) was added in the presence of ionomycin to quench compartmentalized fura2FF completely. Before normalization to the initial fluorescence, the residual signal autofluorescence of the cells was subtracted from the fluorescence signal. Fluorimetric measurements of $\Delta\Psi_m$ were carried out as described previously (Szalai *et al*., 1999). Briefly, suspensions of cells were incubated in permeabilization medium in the presence of 800 nM JC-1 in a fluorimeter cuvette. Fluorescence was monitored using 490 nm excitation/535 nm emission for the monomeric form and 570 nm excitation/595 nm emission for the J-aggregate of JC1 (five data points/s). $\Delta\Psi_m$ is shown as the ratio of the fluorescence of J-aggregate and monomer forms of JC1.

Detection of cytochrome c release by western blotting

At the end of the fluorimetric measurements of $\Delta\Psi_m$ in suspensions of permeabilized cells, cytosol was separated from the membranes by centrifugation at 10 000 *g* for 10 min (data shown in Figure 1). Alternatively, suspensions of the permeabilized cells were rapidly filtered (0.45 μm pore size cellulose acetate membrane; Whatman) using a syringeless filter device (data shown in Figure 5). This approach allowed us to obtain cytosol in <10 s. Supernatant or membrane or filtrate proteins (25 μg) were resolved on a 15% SDS–polyacrylamide gel and western blotting was carried out for cytochrome *c*. To evaluate cytochrome *c* release occurring during cell permeabilization with digitonin, equal volumes of the supernatants obtained using 0, 35 and 100 μg/ml digitonin were loaded onto the gel (Figure 1A, right). Mouse monoclonal anti-cytochrome *c* antibody was used with goat anti-mouse peroxidase conjugate for detection. Bound antibody was detected by enhanced chemiluminescence using the Supersignal reagent (Pierce).

Western blots are representative of three experiments. Every fluorimetry recording shown herein represents the mean response of ~10^7 cells. Furthermore, every recording was repeated at least once using the same cell preparation, and the difference between the parallels was very small in comparison with the differences between control and tcBid described in this study. For each agent (IP_3, Tg, 10Ca), measurements of the effect on control and tcBid-treated cells were obtained using the same cell preparation, and each pair was repeated in 2–7 cell preparations. The data combined from separate experiments are shown as mean ± SE. Significance of differences from the relevant controls was calculated by Student's *t*-test.

Acknowledgements

We would like to thank Drs Suresh K.Joseph and John G.Pastorino for critical reading of the manuscript. This work was supported by grants from the NIH and American Cancer Society (to G.H.). G.H. is a recipient of a Burroughs Wellcome Fund Career Award.

References

Antonsson,B., Montessuit,S., Sanchez,B. and Martinou,J.C. (2001) Bax is present as a high molecular weight oligomer/complex in the mitochondrial membrane of apoptotic cells. *J. Biol. Chem.*, **276**, 11615–11623.

Benz,R. and Brdiczka,D. (1992) The cation-selective substate of the mitochondrial outer membrane pore: single-channel conductance and influence on intermembrane and peripheral kinases. *J. Bioenerg. Biomembr.*, **24**, 33–39.

Bernardi,P. (1999) Mitochondrial transport of cations: channels, exchangers and permeability transition. *Physiol. Rev.*, **79**, 1127–1155.

Beutner,G., Sharma,V.K., Giovannucci,D.R., Yule,D.I. and Sheu,S.S. (2001) Identification of a ryanodine receptor in rat heart mitochondria. *J. Biol. Chem.*, **276**, 21482–21488.

Crompton,M. (1999) The mitochondrial permeability transition pore and its role in cell death. *Biochem. J.*, **341**, 233–249.

Csordás,G. and Hajnóczky,G. (2001) Sorting of calcium signals at the junctions of endoplasmic reticulum and mitochondria. *Cell Calcium*, **29**, 249–262.

Csordás,G., Thomas,A.P. and Hajnóczky,G. (1999) Quasi-synaptic calcium signal transmission between endoplasmic reticulum and mitochondria. *EMBO J.*, **18**, 96–108.

David,G. (1999) Mitochondrial clearance of cytosolic Ca^{2+} in stimulated lizard motor nerve terminals proceeds without progressive elevation of mitochondrial matrix [Ca^{2+}]. *J. Neurosci.*, **19**, 7495–7506.

Desagher,S. and Martinou,J.C. (2000) Mitochondria as the central control point of apoptosis. *Trends Cell Biol.*, **10**, 369–377.

Desagher,S., Osen-Sand,A., Nichols,A., Eskes,R., Montessuit,S., Lauper,S., Maundrell,K., Antonsson,B. and Martinou,J.C. (1999) Bid-induced conformational change of Bax is responsible for mitochondrial cytochrome *c* release during apoptosis. *J. Cell Biol.*, **144**, 891–901.

Du,C., Fang,M., Li,Y., Li,L. and Wang,X. (2000) Smac, a mitochondrial protein that promotes cytochrome *c*-dependent caspase activation by eliminating IAP inhibition. *Cell*, **102**, 33–42.

Eskes,R., Desagher,S., Antonsson,B. and Martinou,J.C. (2000) Bid induces the oligomerization and insertion of Bax into the outer mitochondrial membrane. *Mol. Cell. Biol.*, **20**, 929–935.

Frey,T.G. and Mannella,C.A. (2000) The internal structure of mitochondria. *Trends Biochem. Sci.*, **25**, 319–324.

Green,D.R. and Reed,J.C. (1998) Mitochondria and apoptosis. *Science*, **281**, 1309–1312.

Gross,A., Yin,X.M., Wang,K., Wei,M.C., Jockel,J., Milliman,C., Erdjument-Bromage,H., Tempst,P. and Korsmeyer,S.J. (1999) Caspase cleaved BID targets mitochondria and is required for cytochrome *c* release, while BCL-XL prevents this release but not tumor necrosis factor-R1/Fas death. *J. Biol. Chem.*, **274**, 1156–1163.

Gunter,T.E. and Pfeiffer,D.R. (1990) Mechanisms by which mitochondria transport calcium. *Am. J. Physiol.*, **258**, C755–C786.

Gunter,T.E., Gunter,K.K., Sheu,S.S. and Gavin,C.E. (1994) Mitochondrial calcium transport: physiological and pathological relevance. *Am. J. Physiol.*, **267**, C313–C339.

Hajnóczky,G., Robb-Gaspers,L.D., Seitz,M. and Thomas,A.P. (1995) Decoding of cytosolic calcium oscillations in the mitochondria. *Cell*, **82**, 415–424.

Hajnóczky,G., Csordás,G., Madesh,M. and Pacher,P. (2000) Control of apoptosis by IP3 and ryanodine receptor driven calcium signals. *Cell Calcium*, **28**, 349–363.

Ichas,F. and Mazat,J.P. (1998) From calcium signalling to cell death: two conformations for the mitochondrial permeability transition pore. Switching from low- to high-conductance state. *Biochim. Biophys. Acta*, **1366**, 33–50.

Ichas,F., Jouaville,L.S. and Mazat,J.P. (1997) Mitochondria are excitable organelles capable of generating and conveying electrical and calcium signals. *Cell*, **89**, 1145–1153.

Korsmeyer,S.J., Wei,M.C., Saito,M., Weiler,S., Oh,K.J. and Schlesinger,P.H. (2000) Pro-apoptotic cascade activates BID, which oligomerizes BAK or BAX into pores that result in the release of cytochrome *c*. *Cell Death Differ.*, **7**, 1166–1173.

Krajewski,S. *et al*. (1999) Release of caspase-9 from mitochondria during neuronal apoptosis and cerebral ischemia. *Proc. Natl Acad. Sci. USA*, **96**, 5752–5757.

Kroemer,G. and Reed,J.C. (2000) Mitochondrial control of cell death. *Nature Med.*, **6**, 513–519.

Kröner,H. (1986) Ca^{2+} ions, an allosteric activator of calcium uptake in rat liver mitochondria. *Arch. Biochem. Biophys.*, **251**, 525–535.

Kudla,G., Montessuit,S., Eskes,R., Berrier,C., Martinou,J.C., Ghazi,A. and Antonsson,B. (2000) The destabilization of lipid membranes induced by the C-terminal fragment of caspase 8-cleaved bid is inhibited by the N-terminal fragment. *J. Biol. Chem.*, **275**, 22713–22718.

Lemasters,J.J. *et al*. (1998) The mitochondrial permeability transition in cell death: a common mechanism in necrosis, apoptosis and autophagy. *Biochim. Biophys. Acta*, **1366**, 177–196.

Li,H., Zhu,H., Xu,C.-j. and Yuan,J. (1998) Cleavage of BID by caspase 8 mediates the mitochondrial damage in the Fas pathway of apoptosis. *Cell*, **94**, 491–501.

Li,L.Y., Luo,X. and Wang,X. (2001) Endonuclease G is an apoptotic DNase when released from mitochondria. *Nature*, **412**, 95–99.

Litsky,M.L. and Pfeiffer,D.R. (1997) Regulation of the mitochondrial Ca^{2+} uniporter by external adenine nucleotides: the uniporter behaves like a gated channel which is regulated by nucleotides and divalent cations. *Biochemistry*, **36**, 7071–7080.

Liu,X., Kim,C.N., Yang,J., Jemmerson,R. and Wang,X. (1996) Induction of apoptotic program in cell-free extracts: requirement for dATP and cytochrome *c*. *Cell*, **86**, 147–157.

Luo,X., Budihardji,I., Zou,H., Slaughter,C. and Wang,X. (1998) Bid, a Bcl2 interacting protein, mediates cytochrome *c* release from mitochondria in response to activation of cell surface death receptors. *Cell*, **94**, 481–449.

Lutter,M., Fang,M., Luo,X., Nishijima,M., Xie,X. and Wang,X. (2000) Cardiolipin provides specificity for targeting of tBid to mitochondria. *Nature Cell Biol.*, **2**, 754–761.

Lutter,M., Perkins,G.A. and Wang,X. (2001) The pro-apoptotic Bcl-2 family member tBid localizes to mitochondrial contact sites. *BMC Cell Biol.*, **2**, 22.

Mannella,C.A. (1992) The 'ins' and 'outs' of mitochondrial membrane channels. *Trends Biochem. Sci.*, **17**, 315–320.

Marchetti,P. *et al*. (1996) Mitochondrial permeability transition is a central coordinating event of apoptosis. *J. Exp. Med.*, **184**, 1155–1160.

Marzo,I. *et al*. (1998a) Bax and adenine nucleotide translocator cooperate in the mitochondrial control of apoptosis. *Science*, **281**, 2027–2031.

Marzo,I. *et al*. (1998b) The permeability transition pore complex: a target for apoptosis regulation by caspases and bcl-2-related proteins. *J. Exp. Med.*, **187**, 1261–1271.

Mootha,V.K., Wei,M.C., Buttle,K.F., Scorrano,L., Panoutsakopoulou,V., Mannella,C.A. and Korsmeyer,S.J. (2001) A reversible component of mitochondrial respiratory dysfunction in apoptosis can be rescued by exogenous cytochrome *c*. *EMBO J.*, **20**, 661–671.

Pacher,P. and Hajnóczky,G. (2001) Propagation of the apoptotic signal by mitochondrial waves. *EMBO J.*, **20**, 4107–4121.

Pacher,P., Csordás,G., Schneider,T. and Hajnóczky,G. (2000) Quantification of calcium signal transmission from sarco-endoplasmic reticulum to the mitochondria. *J. Physiol.*, **529**, 553–564.

Rizzuto,R., Brini,M., Murgia,M. and Pozzan,T. (1993) Microdomains with high Ca^{2+} close to IP_3-sensitive channels that are sensed by neighboring mitochondria. *Science*, **262**, 744–747.

Rizzuto,R., Pinton,P., Carrington,W., Fay,F.S., Fogarty,K.E., Lifshitz, L.M., Tuft,R.A. and Pozzan,T. (1998) Close contacts with the endoplasmic reticulum as determinants of mitochondrial Ca^{2+} responses. *Science*, **280**, 1763–1766.

Samali,A., Cai,J., Zhivotovsky,B., Jones,D.P. and Orrenius,S. (1999) Presence of a pre-apoptotic complex of pro-caspase-3, Hsp60 and Hsp10 in the mitochondrial fraction of Jurkat cells. *EMBO J.*, **18**, 2040–2048.

Schendel,S.L., Azimov,R., Pawlowski,K., Godzik,A., Kagan,B.L. and Reed,J.C. (1999) Ion channel activity of the BH3 only Bcl-2 family member, BID. *J. Biol. Chem.*, **274**, 21932–21936.

Scorrano,L., Penzo,D., Petronilli,V., Pagano,F. and Bernardi,P. (2001) Arachidonic acid causes cell death through the mitochondrial permeability transition. Implications for tumor necrosis factor-α apoptotic signalling. *J. Biol. Chem.*, **276**, 12035–12040.

Scorrano,L., Ashiya,M., Buttle,K., Weiler,S., Oakes,S.A., Mannella,C.A. and Korsmeyer,S.J. (2002) A distinct pathway remodels mitochondrial cristae and mobilizes cytochrome *c* during apoptosis. *Dev. Cell*, **2**, 55–67.

Shimizu,S., Narita,M. and Tsujimoto,Y. (1999) Bcl-2 family proteins regulate the release of apoptogenic cytochrome *c* by the mitochondrial channel VDAC. *Nature*, **399**, 483–487.

Susin,S.A. *et al*. (1999a) Molecular characterization of mitochondrial apoptosis-inducing factor. *Nature*, **397**, 441–446.

Susin,S.A., Lorenzo,H.K., Zamzami,N., Marzo,I., Brenner,C., Larochette,N., Prevost,M.C., Alzari,P.M. and Kroemer,G. (1999b) Mitochondrial release of caspase-2 and -9 during the apoptotic process. *J. Exp. Med.*, **189**, 381–394.

Szalai,G., Krishnamurthy,R. and Hajnóczky,G. (1999) Apoptosis driven by IP_3-linked mitochondrial calcium signals. *EMBO J.*, **18**, 6349–6361.

Vander Heiden,M.G. and Thompson,C.B. (1999) Bcl-2 proteins: regulators of apoptosis or of mitochondrial homeostasis? *Nature Cell Biol.*, **1**, 209–216.

Verhagen,A.M., Ekert,P.G., Pakusch,M., Silke,J., Connolly,L.M., Reid, G.E., Moritz,R.L., Simpson,R.J. and Vaux,D.L. (2000) Identification of DIABLO, a mammalian protein that promotes apoptosis by binding to and antagonizing IAP proteins. *Cell*, **102**, 43–53.

Vinogradov,A. and Scarpa,A. (1973) The initial velocities of calcium uptake by rat liver mitochondria. *J. Biol. Chem.*, **248**, 5527–5531.

von Ahsen,O., Renken,C., Perkins,G., Kluck,R.M., Bossy-Wetzel,E. and Newmeyer,D.D. (2000) Preservation of mitochondrial structure and function after Bid- or Bax-mediated cytochrome *c* release. *J. Cell Biol.*, **150**, 1027–1036.

Wang,H.J., Guay,G., Pogan,L., Sauve,R. and Nabi,I.R. (2000) Calcium regulates the association between mitochondria and a smooth subdomain of the endoplasmic reticulum. *J. Cell Biol.*, **150**, 1489–1498.

Wang,K., Yin,X.M., Chao,D.T., Milliman,C.L. and Korsmeyer,S.J. (1996) BID: a novel BH3 domain-only death agonist. *Genes Dev.*, **10**, 2859–2869.

Waterhouse,N.J., Goldstein,J.C., von Ahsen,O., Schuler,M., Newmeyer, D.D. and Green,D.R. (2001) Cytochrome *c* maintains mitochondrial transmembrane potential and ATP generation after outer mitochondrial membrane permeabilization during the apoptotic process. *J. Cell Biol.*, **153**, 319–328.

Wei,M.C., Lindsten,T., Mootha,V.K., Weiler,S., Gross,A., Ashiya,M., Thompson,C.B. and Korsmeyer,S.J. (2000) tBID, a membrane-targeted death ligand, oligomerizes BAK to release cytochrome *c*. *Genes Dev.*, **14**, 2060–2071.

Zamzami,N. *et al*. (2000) Bid acts on the permeability transition pore complex to induce apoptosis. *Oncogene*, **19**, 6342–6350.

Received August 9, 2001; revised February 12, 2002; accepted March 7, 2002